Noname manuscript No.
(will be inserted by the editor)

Image Reproduction with Compensation of Luminance Adaptation

Ufuk Celikcan · Sami Arpa · Tolga Capin

Received: date / Accepted: date

Abstract We introduce an image reproduction model that retargets colors for printing purposes to ensure similar luminance perception under photopic and scotopic vision. Our model is based on the physiological functioning of the rod and cone cells in the retina in varying lighting conditions, so that the human visual system exhibits responses akin to a printed output of the model for different illumination levels. Prior to retargeting, digital color images are converted to spectral representations and their photopic and scotopic luminance responses are obtained. The color retargeting is realized by optimizing our compensation function over the color space. In addition, we present a spatially varying operator to enhance the color coherence over salient regions. Reproduction results demonstrate substantially decreased difference between the two luminance responses. Further, it is validated through psychophysical evaluation that our model on average provides superior recognition rates in dark environments, while keeping the noticeable differences in aesthetic appeal acceptable in well-lit environments.

Keywords purkinje shift · scotopic vision · color appearance · image reproduction

U. Celikcan
Department of Computer Engineering, Hacettepe University, Ankara, Turkey
E-mail: ufuk.celikcan@gmail.com

S. Arpa
School of Computer and Communication Sciences, EPFL, Switzerland
E-mail: msamiarpa@gmail.com

T. Capin
Computer Engineering Department, TED University, Ankara, Turkey
E-mail: tolga.capin@tedu.edu.tr

1 Introduction

Conventional coloring techniques for graphic design, and color adjustment methods for photography depend on the abilities of artists and the capture devices. Neither the artists can fully consider nor the mainstream capturing devices take into account how the printed final image is perceived under low light conditions, although human visual system (HVS) produces different responses at different light levels. The varying viewing conditons likely to occur for a printed material, e.g., dark or poorly-lit outdoor environments for a poster or a billboard, are to be taken into account in order to ensure that the viewer has perceptually similar experiences among them.

The perception of color by HVS is based on the distinct spectral responses of the three types of cone cells, which are short, medium and long cells. In this direction, color space standards, such as CIE XYZ or sRGB, model human color perception assuming that this three dimensional response space is sufficient. On the other hand, the cones are only active in well-lit scenes, while the rod cells, which consist of only a single type of cell, work in dark scenes. Hence, cone-mediated vision (*photopic vision*) presents different spectral responses than rod-mediated vision (*scotopic vision*). This difference, called *Purkinje shift*, is omitted to be modeled in standard color models.

In recent years, several retargeting/calibration processes for digital images have been proposed that manage the appearance of images across different display conditions, including environment lighting. On the other hand, these methods do not take the appearance of printed materials into account. The major difference of printed materials from display outputs is that what we see is carried out only by reflectances, whereas dis-

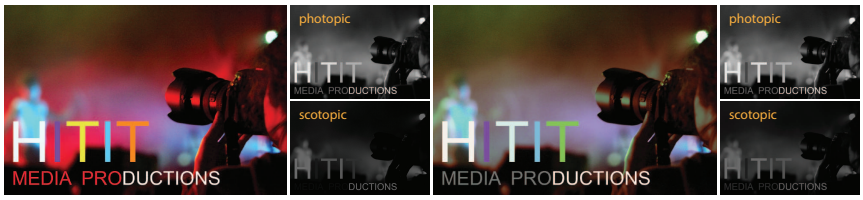

Fig. 1: Our framework optimizes the images to increase their visibility for both day and night vision conditions. A printed image (left) may be perceived quite differently in well-lit and dark environments. We reproduce the image (right) so that it triggers as close as possible luminance response under well-lit and dark scenes. To observe the difference in scotopic luminance response, the image must be printed and shown in a dark environment, i.e., $10^{-1} cd/m^2$.

play devices behave like light sources which results in both cone and rod cell activity in a dark environment, i.e., *mesopic vision*, or only cone activity in a well-lit scene. The printed materials are frequently seen in dark environments such as dark establishments of museums and movie theaters, posters and billboards on the street during night. Hence, how the printed materials are perceived under photopic, mesopic and scotopic vision conditions should be discovered exclusively.

We present a computational model which calculates the difference of perceived luminance under photopic and scotopic vision and utilizes a perceptually based color optimization method which produces standard RGB images that invoke similar luminance response under both well-lit and dark scenes while preserving original colors as much as possible (Figure 1). Our model can help photographers and designers making perceptual color post-processing possible before printing the materials. Previous works focus on how to make a tone-mapping on RGB images so that they appear closer to what HVS would experience in low-light conditions, whereas our goal is processing RGB images to make them visible for both night and day conditions. Additionally, we introduce a local operator which compensates the difference of photopic and scotopic luminance responses with a spatially varying image fidelity approach.

In the rest of the paper, we continue by first giving a short background on HVS; and reviewing color models and the state-of-the-art techniques on the matter. In Section 3, we explain our approach before exhibiting the results of the model in Section 4. Before conclusion, Section 5 presents our user study of the reproduction results.

2 Background and Related Work

HVS contains four different types of photoreceptors, short, medium, and long cone cells, and also rod cells, which outnumber cone cells 20 to 1. Each type of receptor is sensitive to a different distribution of light wavelengths. At very low light levels, visual experience depends solely on the rod cell response. In order to determine color, the visual system compares responses across the three different types of cones with differing absorption spectra. Therefore colors cannot be seen at low light levels where only rod cells are active. Based on response curves of cones (Figure 2), visible spectrum is represented with tristimulus values in a 3D space.

Rods are highly sensitive to light and provide a monochromatic vision in dim lighting. Although the human eye perceives a wide range of light intensities from 10^{-4} to $10^{6} cd/m^2$, rods are eminently functional in dim light, where the range of light intensity is less than $10^{-1} cd/m^2$, called scotopic vision. Cones are not functional under scotopic vision condition, whereas there are cones that only work under photopic vision, at which light intensity is more than $10 cd/m^2$. Both cones and rods work when the light intensity is in the range between 10^{-1} and $10 cd/m^2$, which is called *mesopic vision* [10].

Several research works delved into reproduction of color images considering luminosity adaptation, visual

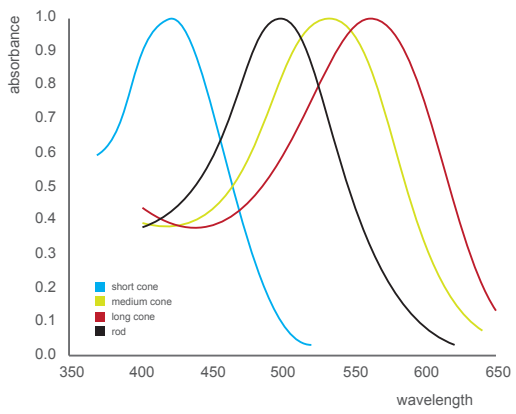

Fig. 2: Spectral responses for rod and cone cells [4].

acuity and color appearance [17]. Ferwerda et al. [6] proposed a global tone mapping operator based on psychophysical experiments. This model can simulate required illumination for an image considering perceived luminance at intensities ranging from photopic vision to scotopic vision. Durand and Dorsey [5] extend the method of Ferwerda et al. by including a blue-shift operator for night scenes, where environment appears to have a tinge of blue during night, and chromatic adaptation. Similarly, Khan and Pattanaik [11] present a model of visual pathways for rod and cone cells to reproduce blue shift for night images. Arpa et al. [1] describe a new type of visual illusion by utilizing the separation between photopic vision and scotopic vision. Wanat and Mantiuk [23] propose a luminance re-targeting method for display screens to match the appearance under different luminance levels.

The basic color theory is established on opponent color model. The theory shows that HVS considers the differences between the responses of cones rather than recording the response of each type of cone. The opponency channels include red-green, blue-yellow, and black-white. It is experienced that rods share the same visual pathway to convey information to the brain. This is shown as the reason of monochromatic perception of rod-mediated vision. Cao et al. [3] investigate rod-mediated changes in color perception and fit a model based on user studies. By using this model, Kirk and O'Brien [12] present a tone-mapping algorithm, which predicts perceived color with a biological model for scotopic and mesopic vision and reproduces the image.

Lightness is a complicated attribute of color to be addressed in a color appearance model (CAM), since the perception of a specific color changes according to the adaptation level of HVS. The adaptation levels are updated considering conditions like the type and intensity of ambient light source (e.g., daylight, electric light), which are tolerated by chromatic adaptation and luminance adaptation. Although HVS operates these automatically, common cameras and CAMs calculate color by considering physical properties. Some recent CAMs such as CIECAM02 [16] provide observing color under different viewing conditions, although they cover a limited range of illumination. Kuang et al. [13] propose an image appearance model which considers the level of adaptation with a spatially varying operator. Similarly Reinhard et al. [18] present a model which calibrates the colors for a wide range of illumination levels to reproduce the appearance of images.

There are several works that focused on color reproduction for printing considering physical model of reflectances. Printing color images with multiple custom inks is a basic problem, which can be solved by methods like gamut-mapping, halftoning and dot gain [21]. Malzbender et al. [14] and Matusik et al. [15] model spatially varying reflectances for printing where the appearance of a print-out changes with lighting conditions (i.e., specular reflection). The method of Hersch et al. [9] creates color images which are printed with fluorescent inks that make them visible only under UV light.

One major limitation of current image reproduction methods for printing, as well as many printing devices, is that they represent images for the case of a single luminance condition. This is a serious drawback since the appearance of real-world printed materials cannot be modeled faithfully by considering a single condition for reflectances, while the previous body of work provides means of retargeting/calibrating images for only a single condition of illumination. In our work, the images are retargeted so that the printed end-product provides similar luminance responses for different illumination levels.

3 Approach

In this work, we search for compensated images that provide similar luminance response under dim-lit environments and well-lit environments while staying faithful to their originals as much as possible. For this, we introduce a novel model that is capable of generating such images through minimization of the total desired energy with respect to the originals, which involves calculation of perceived luminances under photopic and scotopic visions.

Overview This is a perceptual model for reproducing a retargeted image mainly for printing purposes (Figure 3). The principal goal is to keep the resulting image perceptually as-close-as-possible to the input image under different viewing conditions (i.e., luminance range of environment).

The main approach involves three major steps: spectra assessment (Sec. 3.1), luminance response estimation (Sec. 3.2), and color retargeting (Sec. 3.3). Initially, we acquire a spectral representation of the input RGB image so that each RGB triplet for the image has a unique spectrum. Second, using this spectral representation, we measure perceived luminance of the input image under photopic and scotopic viewing conditions. Finally, the image is reproduced to align it for varying viewing conditions. This step automatically retargets the image so that the difference between scotopic and photopic responses is minimized while preventing drastic changes in colors. We also present a locally operating variation of our method at the end of this section (Sec. 3.4).

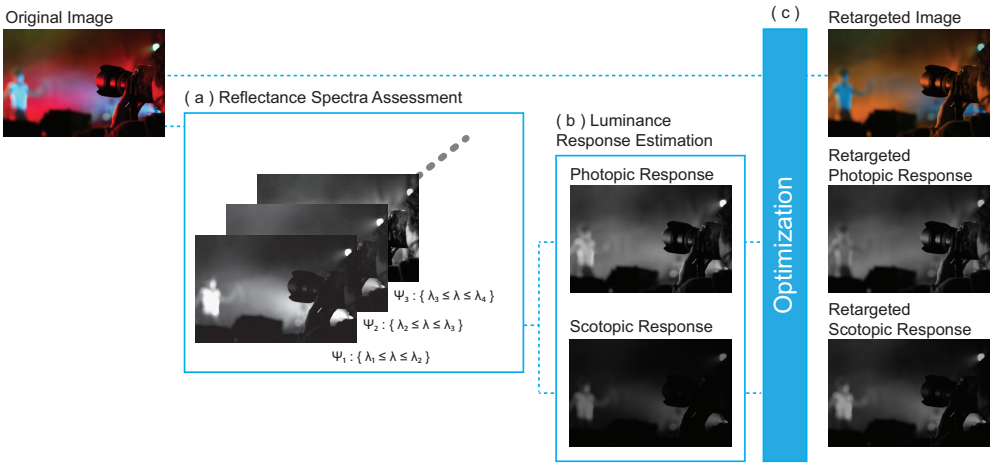

Fig. 3: Our approach. (a) The input is converted to its spectral representation within the desired wavelength ranges. (b) The photopic and scotopic luminance responses are estimated by integrating the spectra against respective standard luminosity curves. (c) Optimization takes the input and the responses to produce the retargeted image.

Definitions Formally, a color retargeted image $h \in \mathbb{R}^2 \rightarrow (0,1)^3$ is a reproduction of input image $p \in \mathbb{R}^2 \rightarrow (0,1)^3$ where it is reproduced using its spectral representation $s \in \mathbb{R}^2 \rightarrow (0,1)^n$ such that $s(\lambda)(\mathbf{x})$ is the spectral distribution of pixel $p(\mathbf{x})$. n is the resolution for spectrum. Photopic luminance response map $r_p \in \mathbb{R}^2 \rightarrow (0,1)$ and scotopic luminance response map $r_s \in \mathbb{R}^2 \rightarrow (0,1)$ are calculated using s.

3.1 Reflectance Spectra Assessment

The main challenge of estimating the spectrum equivalent of a given color is that for any given positive color there exists an infinite number of spectra that can produce that color. While these spectra, known as *metamers*, all reproduce the same color, they are not exact equivalents because when they are used as reflectances and illuminated by non-constant spectra, the results are in general not metamers. Since there is not enough information to pick the right metamer, the goal is, instead, to find a good metamer that is physically plausible.

There have been several methods developed for converting color to spectra [7][20][22]. In this work, we adopt the method developed by Smits [20] which excels in its efficiency and its capability of representing fairly saturated colors by the improvement of including complementary colors in the conversion. The method makes use of piecewise constant spectra, as the relatively narrow and non-overlapping support of the basis functions cover all wavelengths in the visible spectrum and, thus, the filtering issues raised by point samples are handled automatically.

A good metamer $s(\mathbf{x})$ for $p(\mathbf{x})$ is smooth and its basis functions yield $\forall\lambda\ s(\lambda)(\mathbf{x}) \geq 0$. The method regards the differences between adjacent basis functions as a measure of smoothness. For the sake of computational efficiency, the linear nature of the conversion is exploited and only the spectra for red, green, blue, cyan, magenta, yellow, and white are created, as it is possible to represent any color as a sum of white, and one of cyan, magenta, or yellow, plus one of red, green, or blue. The conversion algorithm proceeds by removing as much of the wider spectra (first white, then one of cyan, magenta, or yellow) as possible before converting the residual using the red, green, or blue spectra.

3.2 Luminance Response Estimation

After having acquired spectral data s from the input image p, we determine the luminance response of the image under photopic and scotopic lighting conditions. In order to convert the spectral image to luminosity space, the spectral distribution of each pixel is integrated against the standard luminosity curve [2]. That is, for a pixel with spectrum $s(\lambda)(\mathbf{x})$ and the normalized luminance efficiency functions $V_P(\lambda)$ and $V_S(\lambda)$ for photopic and scotopic conditions, respectively, the normalized luminance responses r_p and r_s can be estimated as

$$r_p(\mathbf{x}) = \kappa_1 \int_\lambda s(\lambda)(\mathbf{x}) V_P(\lambda)\, d\lambda \tag{1}$$

and

$$r_s(\mathbf{x}) = \kappa_2 \int_\lambda s(\lambda)(\mathbf{x}) V_S(\lambda)\, d\lambda \tag{2}$$

where κ_1 and κ_2 are normalization factors.

3.3 Color Retargeting

In the final step, we find optimum colors, which are coherent with the original colors and reveal smaller difference of r_p and $r_s$values, to construct the final image h. Our solution space includes all noticeable colors C by HVS.

For a given color $p(\mathbf{x})$, we first define an energy term $E_f = \left\|p^{Lab}(\mathbf{x}) - h^{Lab}(\mathbf{x})\right\|^2$ that measures the distance between $p(\mathbf{x})$ and the candidate color $h(\mathbf{x})$. Both of them are converted to CIE-Lab from RGB values. This term is required to preserve image fidelity to some extent and provide pixel-to-pixel coherence. It ensures selecting a similar solution to original color as-much-as-possible.

We also need another measure to evaluate the change in the perceived luminance under photopic vision between $r_p(\mathbf{x})$ and $r_p^h(\mathbf{x})$, where $r_p^h(\mathbf{x})$ is the photopic luminance response for $h(\mathbf{x})$ acquired using Equation 1. For this we define $E_p = \left\|r_p(\mathbf{x}) - r_p^h(\mathbf{x})\right\|^2$ which controls the proximity of solution to original photopic luminance response.

Finally, we define our last energy term $E_c = \left\|r_p^h(\mathbf{x}) - r_s^h(\mathbf{x})\right\|^2$ to assess the dissimilarity of the perceived luminances of h for photopic vision and scotopic vision, where $r_s^h(\mathbf{x})$ is scotopic luminance response for $h(\mathbf{x})$ acquired using Equation 2. The compensation of luminance response is ensured by E_c.

The combination of the energy terms E_f, E_p and, E_c weighted with α_1, α_2 and, α_3, respectively, defines the total energy E_t s.t. $E_t = \alpha_1 E_f + \alpha_2 E_p + \alpha_3 E_c$, where $\{\alpha_1, \alpha_2, \alpha_3\} \in [0, 1]$.

By carrying out the optimization with our goal

$$\arg\min_{h(\mathbf{x})\in C} E_t, \tag{3}$$

i.e., searching for h over space C for which E_t attains its minimum value, we reach the optimal retargeted color $h(\mathbf{x})$ for each given CIE-Lab value $p(\mathbf{x})$. Hence, the overall optimized cost for the given image Ω becomes

$$E(\Omega) = \int_{\Omega} \left[\min_{h(d\Omega)\in C} E_t\right] d\Omega, \tag{4}$$

which returns the final color retargeted image h.

3.4 Local Operator

We propose an extension of our main approach (global operator) as a local operator. With this local operator, we provide a spatially varying retargeting that seeks to keep significant regions of the image more color coherent with the input and to compensate the regions with large perceived photopic and scotopic response difference more intensively towards bringing the responses closer.

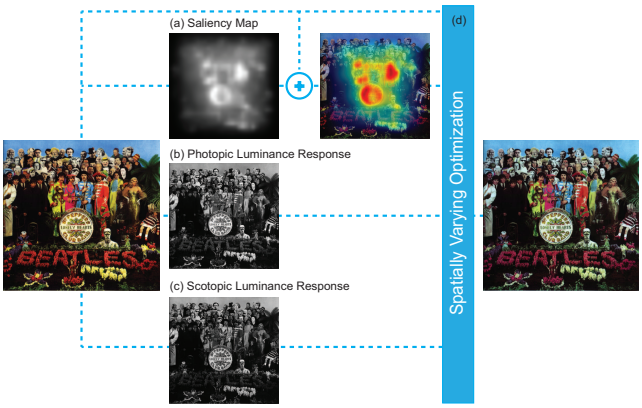

Fig. 4: Overview of the local operator. The photopic luminance response (b) and the scotopic luminance response (c) of the input are estimated; and its saliency map (a) is calculated. The saliency map matched with the input is fed into the spatially varying optimization (d) along with the input image and the responses in order to produce the spatially calibrated output.

Let the energy of the difference between photopic response $r_p(\mathbf{x})$ and the scotopic response $r_s(\mathbf{x})$ of $p(\mathbf{x})$ be denoted as $E_c^p = \|r_p(\mathbf{x}) - r_s(\mathbf{x})\|^2$ and the saliency of $p(\mathbf{x})$ be denoted as $w(\mathbf{x}) \in [0, 1]$ which is calculated according to *Graph-Based Visual Saliency* method [8]. Then, the locally varying total energy is defined as $E_t^l(\mathbf{x}) = (\alpha_1 E_f + \alpha_2 E_p)\,\beta(\mathbf{x}) + \alpha_3 E_c/\beta(\mathbf{x})$, where $\beta(\mathbf{x})$ is $e^{(w(\mathbf{x})-E_c^p)}$.

Replacing E_t in Equation 4, $E_t^l(\mathbf{x})$ is minimized with a chosen weight set $\boldsymbol{\alpha}$, thus resulting in a spatially varying optimization. This way, optimization behaves in accordance with the goals described above, e.g., it is heavily biased towards minimizing E_f and E_p within regions with high saliency and low E_c^p, and heavily biased towards minimizing E_c where it is vice versa. Figure 4 shows the overview of the local operator with a sample input image and the output.

4 Results and Discussion

The optimization (Equation 3) is realized by using *fmincon* function of MATLAB with *active-set* algorithm. Figure 5 demonstrates a series of results created with several sets of weights $\boldsymbol{\alpha} : \{\alpha_1, \alpha_2, \alpha_3\}$ by our main method in comparison to the original image. The sets

of $\boldsymbol{\alpha}$ and the full list of numerical results pertaining to the figure are given in Table 1. Part of the measures used in evaluation of the results are defined as the root-mean squared difference between :

- normalized photopic and scotopic luminance responses of the corresponding image ($RMSD_{P/S}$).
- normalized photopic luminance responses of the original image and the corresponding image ($RMSD_{P/PO}$).
- normalized scotopic luminance responses of the original image and the corresponding image ($RMSD_{S/SO}$).

The results are also compared in terms of *just-noticeable difference* (JND), converted from ΔE color differences. JND color model is defined as characterized by the limitations of HVS [19] s.t. an average observer can detect a difference between two colors if they are at least one JND apart from each other. Our JND-related measures are μ_{JND}, mean JND of the corresponding image with respect to the original image, and max_{JND}, maximum JND of the corresponding image with respect to the original image.

In Figure 5, it is observed that the retargeting can be biased towards keeping the result more faithful to the original, i.e., having less JND, by setting weights of E_f and E_p higher than that of E_c. It is also evident that the retargeting can be made to focus on bringing the perceived photopic and the scotopic luminance responses of the resulting image as close as possible by increasing the weight of E_c relative to others.

On the other hand, one also sees that it is possible to compromise on both means, e.g., by setting all the weights equal, as in row (d) with $\boldsymbol{\alpha} : \{1, 1, 1\}$, and achieve a result that is still color coherent with the original while significantly reducing $RMSD_{P/S}$. In this case with the test image in row (a), the retargeted image is only $\mu_{JND} = 1.67$ JND apart and $RMSD_{P/S}$ is reduced to 63.4% of the original. In Figure 5 of the supplementary material, results with other test images demonstrate reductions in $RMSD_{P/S}$ between 39.60% and 83.07%, further illustrating the degree that our model is able to attain in decreasing the difference betweeen photopic and scotopic illumination responses.

With the local operator, it is possible to achieve better color fidelity on salient image regions while $RMSD_{P/S}$ is kept considerably reduced, as demonstrated in Figure 6. When the test image is retargeted by our regular approach with weights $\boldsymbol{\alpha} : \{1/3, 1, 1\}$, the resulting image has $\mu_{JND} = 2.16$ JND, $max_{JND} = 14.85$ JND, and its $RMSD_{P/S}$ is reduced to 0.00279 from 0.00706 of the test image. By using the local operator with the same weight set, the result has its max_{JND} reduced to 8.11 JND, its μ_{JND} reduced to 0.72 JND, while its $RMSD_{P/S}$ increased to 0.00488, still well below the original.

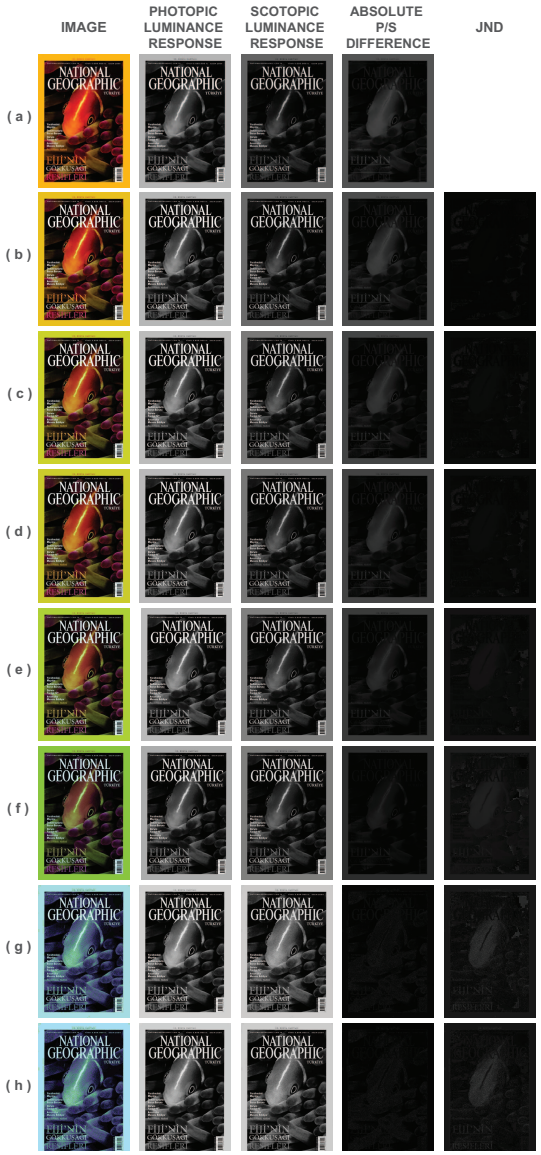

Fig. 5: The first row (a) shows the original image with its photopic and scotopic luminance responses and the absolute difference between the two responses. From the second row (b) onward, the results created with varying sets of $\boldsymbol{\alpha}$ are shown with JND of the resulting image with respect to the original in the last column. Note: the results presented here are advised to be observed via the digital version of the paper for the sake of a more thorough examination.

The local operator results show noticeable improvement in color coherence on high-saliency regions. The results also clearly indicate a trade-off between the average visual fidelity to the original input and the overall quality of the perceived scotopic luminance. This is further exposed by comparing the resulting $RMSD_{P/PO}$

row	α	$RMSD_{P/S}$	$RMSD_{P/PO}$	$RMSD_{S/SO}$	μ_{JND}	max_{JND}
a	-	0.030997	-	-	-	-
b	{ 0.75, 1.0, 0.25 }	0.026193	0.000046	0.000403	0.84	6.73
c	{ 0.25, 1.0, 0.25 }	0.020453	0.000419	0.002878	1.60	7.16
d	{ 1.0, 1.0, 1.0 }	0.019648	0.000131	0.002162	1.67	7.16
e	{ 0.25, 0.25, 0.5 }	0.014865	0.000289	0.004958	2.52	8.15
f	{ 0.25, 0.0, 1.0 }	0.008567	0.000595	0.004058	3.87	8.47
g	{ 0.0, 0.5, 0.75 }	0.002381	0.005236	0.057885	3.64	13.12
h	{ 0.0, 0.1, 1.0 }	0.002251	0.005389	0.057263	3.43	12.74

Table 1 The table lists $\boldsymbol{\alpha}$ used, as well as $RMSD_{P/S}$, $RMSD_{P/PO}$, $RMSD_{S/SO}$, μ_{JND}, and max_{JND}, of the images in corresponding rows in Figure 5.

and $RMSD_{S/SO}$. Applying the local operator to the test image in Figure 6 decreases $RMSD_{P/PO}$ from 0.00800 of the regular result to 0.00030, and $RMSD_{S/SO}$ from 0.00874 to 0.00058.

Limitations Our approach has several limitations. Although we use E_f term to provide pixel to pixel color coherence, the result may have noise for small values of α_1, which also cause dramatic color changes. Therefore, the use of too small α_1 value (lower than 0.1) is to be avoided. Noise could be reduced using a region based optimization for small α_1 values. We try to keep the color fidelity to some extent, however, this is not fully achieved as a consequence of the inherent nature of our aim, i.e., actualizing similar perceived photopic and scotopic vision response. To achieve an observable compensation, significant change in original color is required since visual acuity is very low for scotopic vision conditions.

Furthermore, applying our method for images having small size is to no avail, since the decrease in visual acuity prevents the observation of difference in dark scenes. We suggest using our model for large images such as posters and billboards. The model could be enhanced providing a region-specific artistic control so that users can choose a compensation level depending on the region.

Fig. 6: Comparison of global operator and local operator. Clockwise from the top left: The first image is the input test image; the second is the result with the global operator; the third is the result with the local operator; and the fourth is the saliency map appended input.

5 Study

In order to evaluate the psychophysical validity of our model, a recognition study and an aesthetic appeal study were conducted with 7 subjects, all of whom were naive to the specific purpose of the study. For the recognition study, stimuli printed on A3 matte paper were shown to the participants in a dark room (0.01 cd/m^2). The stimuli were 10 pairs of images, each pair consisting of an original test image and its reproduction by our model[1]. In each trial, a subject was presented with a single pair of images, with the order of the original image and the reproduction randomized, and was asked the following two-alternative forced-choice question: "Which of the two images reveal more details?".

The results (Table 2) of the recognition study significantly ($\rho < 0.001$, with respect to chance probability 50%, pairwise binomial) exhibit that, on average, the images reproduced by our model are perceived to be showing more details in dark room conditions (scotopic vision), than the original images. That is, according to the results, the reproductions are chosen over their original counterparts in 80% of the trials with a standard deviation of 0.13 among subjects' choices. In further detail, it is seen that some of the reproductions (IDs: 2, 5, 6, 9) are chosen by all subjects. Only in two pairs (IDs: 3, 8), the original is chosen by more subjects than its reproduction. This is due to the fact that each of those two original images have scotopic response inherently close to photopic response, therefore the method's impact is diminished.

The study of aesthetic appeal was conducted in a room with standard office lighting (photopic vision). This time, a subject was shown the set of 20 images, from the same 10 pairs of stimuli, in a random order and asked to rate each image individually in terms of aesthetic appeal on a Likert scale of 0 to 5. According to the results, the details of which are given in the supplementary material, the overall mean score of the reproduced images is 2.83 while it is 3.54 for the originals. The signed difference of the mean scores per image pair ranges between 0.07 and 1.86, except for one pair where it is −0.43, the negative value indicating the reproduction is rated higher on average. We find the overall signed mean score difference of 0.71 to be acceptable, especially in view of the assumption that it would dial down as lighting conditions get darker.

[1] Due to space limitations, complete details of the study procedures and the stimuli are provided in the supplementary material of this paper.

a)

Subject ID	1	2	3	4	5	6	7
Choice Ratio	0.7	0.9	0.7	1.0	0.7	0.7	0.9

b)

Image Pair ID	1	2	3	4	5	6	7	8	9	10
Choice Ratio	0.65	1.00	0.49	0.84	1.00	1.00	0.98	0.35	1.00	0.84

Table 2 Results of the recognition study. a) Ratios of reproduction results chosen over original images in all image pairs per subject. b) Ratios of the reproduction result choices by subjects over the original image per image pair.

6 Conclusion

We believe that the proposed model, which reproduces an image to compensate for possible loss of visual information occurring due to poor dark response, can be beneficial in creating large printed images, particularly, posters and billboards which are often observed under vastly varying lighting conditions.

Although the model retargets an image by preserving color fidelity to a degree, resulting color changes may not be always artistically plausible. To remedy this, we also proposed a local operator which changes the compensation level according to spatial significance, i.e., saliency information, and the distance of the responses.

The numerical evaluation of the results indicate that the model succeeds in closing the gap between photopic and scotopic luminance responses remarkably while increasing their visibility in dark environments. The two user studies validate these findings to a great extent. The recognition study reveals that for images with poor scotopic vision response, the proposed model can reproduce compensated images that are perceived with significantly richer detail in dark scenes. The aesthetic appeal study shows that while these reproductions are in general found to be less aesthetically appealing, the measured change in appeal is usually acceptable.

References

1. Arpa, S., Ritschel, T., Myszkowski, K., Çapın, T., Seidel, H.P.: Purkinje images: Conveying different content for different luminance adaptations in a single image. In: Computer Graphics Forum. Wiley Online Library (2014)
2. Bureau Central de la CIE: In: CIE Proceedings 1951. Vol. 1, Sec. 4; Vol. 3, Page 37 (1951)
3. Cao, D., Pokorny, J., Smith, V.C., Zele, A.J.: Rod contributions to color perception: linear with rod contrast. Vision research **48**(26), 2586–2592 (2008)
4. Dartnall, H., Bowmaker, J., Mollon, J.: Human visual pigments: microspectrophotometric results from the eyes of seven persons. Proceedings of the Royal society of London. Series B. Biological sciences **220**(1218), 115–130 (1983)
5. Durand, F., Dorsey, J.: Interactive tone mapping. In: Proceedings of the Eurographics Workshop on Rendering Techniques, pp. 219–230 (2000)
6. Ferwerda, J.A., Pattanaik, S.N., Shirley, P., Greenberg, D.P.: A model of visual adaptation for realistic image synthesis. In: Proceedings of the 23rd annual conference on Computer graphics and interactive techniques, pp. 249–258. ACM (1996)
7. Glassner, A.S.: How to derive a spectrum from an rgb triplet. Computer Graphics and Applications, IEEE **9**(4), 95–99 (1989)
8. Harel, J., Koch, C., Perona, P.: Graph-based visual saliency (2007)
9. Hersch, R.D., Donzé, P., Chosson, S.: Color images visible under uv light. In: ACM Transactions on Graphics (TOG), vol. 26, p. 75. ACM (2007)
10. Hood, D.C., Finkelstein, M.A.: Sensitivity to light. Terminology **5**, 27 (1986)
11. Khan, S.M., Pattanaik, S.N.: Modeling blue shift in moonlit scenes by rod cone interaction. Journal of VISION **4**(8) (2004)
12. Kirk, A.G., , O'Brien, J.F.: Perceptually based tone mapping for low-light conditions. ACM Transactions on Graphics **30**(4), 42:1–10 (2011). Proceedings of ACM SIGGRAPH 2011, Vancouver, BC Canada
13. Kuang, J., Johnson, G.M., Fairchild, M.D.: icam06: A refined image appearance model for hdr image rendering. Journal of Visual Communication and Image Representation **18**(5), 406–414 (2007)
14. Malzbender, T., Samadani, R., Scher, S., Crume, A., Dunn, D., Davis, J.: Printing reflectance functions. ACM Transactions on Graphics (TOG) **31**(3), 20 (2012)
15. Matusik, W., Ajdin, B., Gu, J., Lawrence, J., Lensch, H., Pellacini, F., Rusinkiewicz, S.: Printing spatially-varying reflectance. In: ACM Transactions on Graphics (TOG), vol. 28, p. 128. ACM (2009)
16. Moroney, N., Fairchild, M., Hunt, R., Li, C., Luo, M.R., Newman, T.: The ciecam02 color appearance model (2002)
17. Reinhard, E., Heidrich, W., Debevec, P., Pattanaik, S., Ward, G., Myszkowski, K.: High dynamic range imaging: acquisition, display, and image-based lighting. Morgan Kaufmann (2010)
18. Reinhard, E., Pouli, T., Kunkel, T., Long, B., Ballestad, A., Damberg, G.: Calibrated image appearance reproduction. ACM Transactions on Graphics (TOG) **31**(6), 201 (2012)
19. Sharma, G., Bala, R.: Digital color imaging handbook. CRC press (2010)
20. Smits, B.: An rgb-to-spectrum conversion for reflectances. J. Graph. Tools **4**(4), 11–22 (1999). DOI 10.1080/10867651.1999.10487511
21. Stollnitz, E.J., Ostromoukhov, V., Salesin, D.H.: Reproducing color images using custom inks. In: Proceedings of the 25th annual conference on Computer graphics and interactive techniques, pp. 267–274. ACM (1998)
22. Sun, Y., Fracchia, F.D., Calvert, T.W., Drew, M.S.: Deriving spectra from colors and rendering light interference. IEEE Computer Graphics and Applications **19**(4), 61–67 (1999)
23. Wanat, R., Mantiuk, R.K.: Simulating and compensating changes in appearance between day and night vision. Proceedings of SIGGRAPH 2014 **33**, 147 (2014)